Journal of Peptide Science
J. Pept. Sci. 2008; **14**: 496–502
Published online 17 December 2007 in Wiley InterScience (www.interscience.wiley.com). DOI: 10.1002/psc.970

JOURNAL OF PEPTIDE SCIENCE

Fuscopeptins, antimicrobial lipodepsipeptides from *Pseudomonas fuscovaginae*, are channel forming peptides active on biological and model membranes‡§

M. CORAIOLA,[a] R. PALETTI,[a] A. FIORE,[b] V. FOGLIANO[b] and M. DALLA SERRA[a]*

[a] FBK & CNR Istituto di Biofisica, via alla Cascata 56/C, I-38100 Povo (Trento), Italy
[b] Dipartimento di Scienza degli Alimenti, Università di Napoli Federico II, 80138 Napoli, Italy

Received 25 June 2007; Revised 14 September 2007; Accepted 1 October 2007

Abstract: FP-A and FP-B are LDPs produced by the plant pathogen *Pseudomonas fuscovaginae*. As expected from their primary structure, they shared a similar mechanism of action with the better characterized SPs, synthesized by strains of *Pseudomonas syringae* pv. *syringae*. Indeed, they displayed hemolytic activity on human erythrocytes and were able to induce calcein release from LUVs: the effect was dependent on the concentration of the FPs and the lipid composition of the liposome and, in particular, it increased with the SM content of the membrane. The permeabilizing activity was further investigated on PLMs. FPs were able to open pores on pure POPC membranes. Pore opening was strongly voltage dependent: by switching the potential from negative to positive values, an increase in the absolute amplitude of transmembrane current was induced with simultaneous closure of pores. In 0.1 M KCl both FPs' pores had a conductance of 4 and 9 pS at −140 mV and +140 mV, respectively. Studies on ion selectivity indicated that FPs formed cation-selective channels. Copyright © 2007 European Peptide Society and John Wiley & Sons, Ltd.

Keywords: lipodepsipeptide; *Pseudomonas fuscovaginae*; liposome; hemolysis; lipid bilayer; ion channel; voltage gating; antimicrobial peptide

INTRODUCTION

FP-A and FP-B are LDPs produced by virulent strains of *Pseudomonas fuscovaginae*, the causal agent of the disease known as 'sheath brown rot' of cultivated and wild *Gramineae*. Their structure, as determined by [1], is strictly related to that of peptin-like LDPs which include SPs, synthesized by phytopathogenic strains of *Pseudomonas syringae* pv. *syringae* [2,3], tolaasins, produced by the mushroom infecting saprophytic *Pseudomonas tolaasii* [4,5], and corpeptins from the tomato pathogen *Pseudomonas corrugata* [6]. Together with the group of the smaller nonapeptides (among them SRE produced by strains of *P. syringae* pv. *syringae* is the best studied [7,8]), they show the characteristic LDP structure: a 3-hydroxy substituted unbranched fatty acid chain is linked to the *N*-terminal of a peptide moiety that is closed in a lactone macrocycle at the *C*-terminus (Figure 1). The peptidic portion is often composed of unusual residues and with D-chirality. Nonapeptides consist of a nine-residue acylated peptide that is closed between the first and the last residue forming a cyclic structure. The peptin-like LDPs are bigger and more complex: the peptide moiety is again acylated at the *N*-terminus and, depending on the LDP, is composed of 18–25 amino acids with a cyclic ring of five or eight residues at the *C*-terminus. The main difference between FPs and the other peptin-like LDPs lies in the primary structure: in the *N*-terminal region of the peptide it bears a sequence of ten D-amino acids (Pro^2-Val^{13}) rich in Ala and Val residues, only interrupted by two L-amino acids, a Leu and Gly at position 3 and 9, respectively. It also contains a 2,3-dehydro-aminobutyric acid (ΔBut) residue at positions 1 and 14 and a 2,4-diaminobutyric acid (Dab) at positions 17 and 18 with L and D configuration, respectively. Finally, a lacton ring of five residues is formed between the hydroxyl of D-Thr^{15} and the *C*-terminal L-Phe^{19}. The two FPs are homologues differing only in their fatty acid moieties: the *N*-terminus is in turn acylated by 3-hydroxyoctanoate in FP-A and 3-hydroxydecanoate in FP-B [1].

FPs are involved in disease development; indeed these molecules, mixed with the lipodepsinonapeptide ST concurrently synthesized by pathogenic strains of *P. fuscovaginae*, can reproduce the same symptoms as those observed in diseased plants [9]. The biological activity of FPs is close to those of SPs: they induce

Abbreviations: Cho, cholesterol; FPs, fuscopeptins; FP-A, fuscopeptin A; FP-B, fuscopeptin B; HRBCs, human red blood cells; LDPs, lipodepsipeptides; LUVs, large unilamellar vesicles; PLMs, planar lipid membranes; POPC, 1-Palmitoyl-2-Oleoyl-sn-Glycero-3-Phosphocholine; PC, egg phosphatidylcholine; SM, sphingomyelin; SPs, syringopeptins; SP25A, syringopeptin 25A; SP22A, syringopeptin 22A; SRE, syringomycin E; ST, syringotoxin; Tol, tolaasin I.

*Correspondence to: M. Dalla Serra, FBK & CNR Istituto di Biofisica, via alla Cascata 56/C, I-38100 Povo (Trento), Italy;
e-mail: mdalla@fbk.eu

‡ This article is part of the Special Issue of the Journal of Peptide Science entitled "2nd workshop on biophysics of membrane-active peptides".

§ This paper is dedicated to the memory of Gianfranco Menestrina.

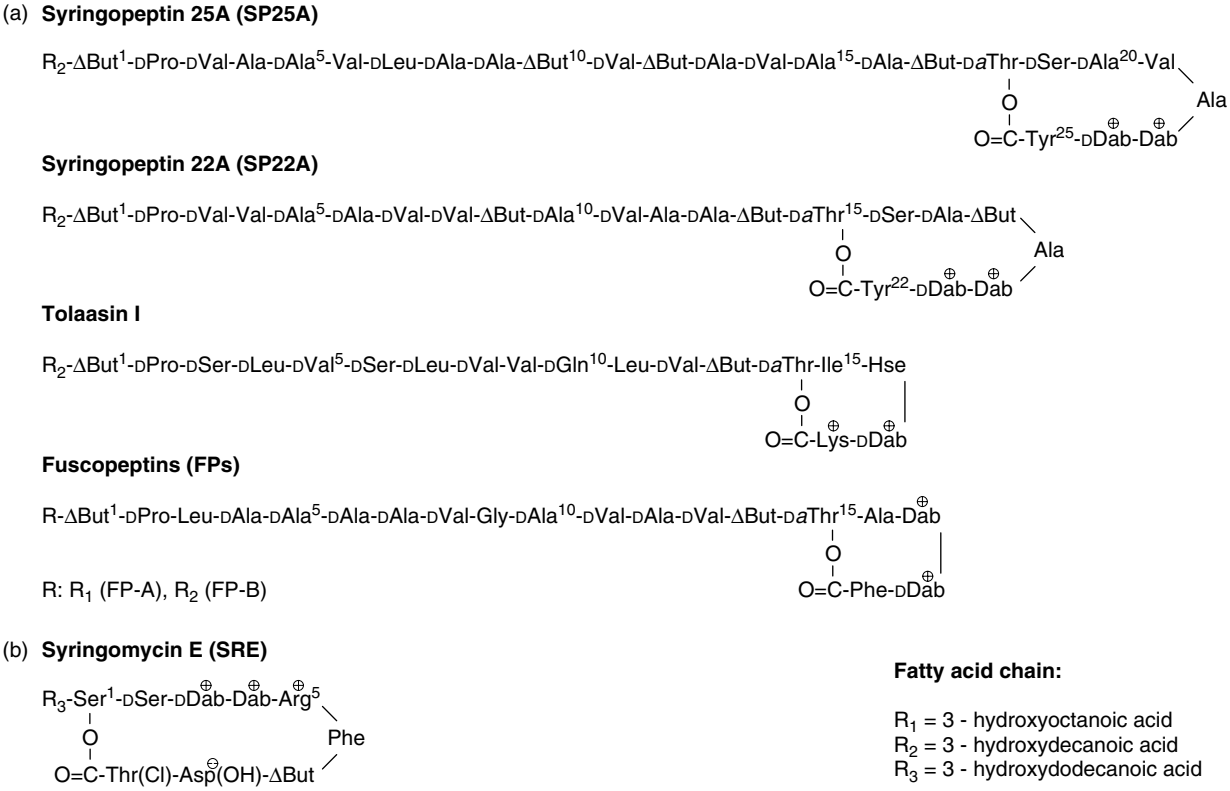

Figure 1 Structure comparison inside members of the two groups of LDPs:LDPs with a peptin-like structure (a) and nonapeptides (b). For the sake of simplicity in (a), beside FPs, we reported the primary structure of SP25A and SP22A (among SPs) and Tol (among tolaasins), while in (b) the SRE structure is shown. Nonstandard amino acids are indicated as follows: ΔBut, 2,3-dehydro-2-aminobutyric acid; *a*Thr, *allo* threonine; Dab, 2,4-diaminobutyric acid; Hse, homoserine; Asp(OH), 3-hydroxy aspartic acid; Thr(Cl), 4-chlorothreonine. Electrically charged amino acids are marked with the corresponding plus or minus symbols; aminoacids with D configuration are specified.

damage of plant tissues and are active in antifungal bioassays [1,9]. In particular, Batoko *et al.* [9] showed the ability of both FPs to inhibit H^+ – ATPase activity of rice membranes. However, no currently available data could clearly explain FPs activity at a molecular level.

Because of the structural relationship between FPs and the other peptin-like LDPs, we supposed a similar mechanism of action, mediated by opening of pores in the plasma membrane. In the present work, we first assessed this by performing experiments with large unilamellar lipid vesicles loaded with calcein and by testing the effects of FPs on red blood cells. Secondly, by using the planar lipid bilayer technique, we investigated the electrophysiological properties of these lesions demonstrating their ability to open ion conductive pores into membranes.

MATERIALS AND METHODS

Chemicals

Lipids used were PC, POPC and SM from Avanti Polar Lipids (Alabaster, AL, USA), Cho from Fluka. Calcein, EDTA, and Sephadex G-50 were from Sigma, Triton X-100 from Merck.

Fuscopeptin Isolation

FPs were obtained from a culture filtrate of *P. fuscovaginae* as described by [1]. The isolation procedure is briefly given here. Crude extracts were fractionated by reversed-phase HPLC on a preparative Aquapore RP300 column (220 × 10 mm, 7 μm internal diameter; Applied Biosystems, Framingham, MA, USA) using a model 200LC pump (PerkinElmer, Fremont, CA, USA) and a model SP-10AVvp UV-VIS detector (Shimadzu, Japan). Flow rate was 4 ml/min and a stepwise gradient of Phase A (TFA 0.1%) and Phase B (Acetonitrile–isopropanol 3 : 1; TFA 0.2%) were used to elute the bioactive compounds. Peaks were manually collected and the freeze-dried material was used for further characterization. Purity was checked by MS and the toxin was quantified by HPLC as reported in [1,10].

Permeabilization of Unilamellar Lipid Vesicles

The permeabilizing activity of FPs was assayed by measuring the release of calcein from LUVs as previously described by [11]. Briefly, LUVs were prepared at 4 mg/ml lipid concentration, by extrusion through two stacked polycarbonate filters with 100 nm pores. During preparation, they were loaded with calcein at a self-quenching concentration (80 mM). The diameter of the vesicles was assessed by dynamic light scattering (Zetasizer 1000-HS_A, Malvern Instruments, Malvern, UK) as reported in [12]. The external nonencapsulated calcein

DOI: 10.1002/psc

was removed by washing the suspension of vesicles through Sephadex G50 minicolumns.

The permeabilizing assay on vesicle of different lipid composition (as detailed in Results) was performed at room temperature using a kinetic microplate fluorimeter reader (Fluostar, BMG, Offenburg, Germany), as already reported [11]. FPs were 2-fold serially diluted in 140 mM NaCl, 20 mM Mes, 1 mM EDTA, pH 6.0 (hereafter buffer A). Aliquots of washed LUVs were introduced into each well to a 6–8 μM final lipid concentration, in 200 μl final volume of buffer A. The percentage of permeabilization after 1 h (R%) was calculated as $(F_{fin} - F_{in})/(F_{max} - F_{in}) \times 100$, where F_{in} and F_{fin} represent the initial and final value of fluorescence before and after peptide addition, respectively. F_{max} is the maximum calcein release and was obtained by adding 1 mM Triton X-100.

RBC Hemolysis

Hemolytic activity of FPs on HRBCs was determined turbidimetrically at 650 nm with a 96-well microplate reader (UVmax, Molecular Devices, Sunnyvale, CA) as described previously [11]. Briefly, HRBCs were prepared from fresh venous blood by washing 3 times in 0.85% NaCl. FPs were 2-fold serially diluted and the reaction was started by adding about 2.4×10^6 cells/well in a 200 μl final volume of buffer A, corresponding to an initial absorbance value (A_{650}) of 0.1 OD.

The extent of hemolysis after 1 h (HL%) was calculated as $(A_i - A_f)/(A_i - A_w) \times 100$, where A_i and A_f are the absorbance at the beginning and end of the reaction, respectively and A_w is that obtained after hypotonic lysis with the pure water.

Planar Lipid Membranes

Electrical properties of the pore formed by FPs were measured on PLMs as reported by [13]. Briefly, a membrane composed of POPC was generated by apposition of two monolayers on both sides of a hole bathed symmetrically by 2 ml of 10 mM Mes, 100 mM KCl pH 6.0 (hereafter buffer B). FPs (either FP-A or FP-B) were added to the *cis*-side of stable preformed membranes at room temperature; *trans*-side was grounded. Pore opening events were recorded as discrete steps of currents by using a patch-clamp amplifier (3900 A of Dagan Corporation, Minneapolis, MN, USA) equipped with the 3910 expander module for PLM application. Membrane current was filtered at 200 Hz and directly acquired by a computer using Clampex 8 software (Axon instruments, Foster City, CA, USA).

RESULTS AND DISCUSSION

Permeabilization of Unilamellar Lipid Vesicles and Hemolytic Activity

As expected from the high structural similarity, the lytic activity found for FPs on both synthetic and biological membranes reproduced well that observed for other peptin-like LDPs. FPs were able to permeabilize model membranes comprised of purified lipid components only. In fact, the addition of these compounds to a solution containing LUVs loaded with calcein at a self-quenching concentration, promoted the release of the dye as indicated by the fluorescence increase (Figure 2). Membrane permeabilization after addition of peptides occurred without affecting the size of vesicles, as checked by dynamic light scattering (data not shown), excluding the possibility of a detergent-like action, for all the lipid composition and toxin concentrations tested. Besides the concentration of the FPs, the extent of permeabilization was also dependent on the lipid composition of the vesicle (Figure 2). The activities of both toxins, as derived from dose dependence experiments (Figure 3) and expressed as $1/C_{50}$, were reported for three different compositions of LUVs in Table 1. The activity was decreased if Cho was present as a lipid component in the membrane. This is a common characteristic as already described for other related LDPs (Table 1) such as SPs [11,14], Tol [15]; it again confirmed the different activity of peptins with respect to the group of the smaller nonapeptides, which showed a clear preference for sterols [11,14,16–19]. These differences could have physiological implications: the peptin-like LDPs are more effective on LUVs reproducing lipid composition typical of plant cell membranes (phospholipids and SM), while the nonapeptides prefer sterol-containing LUVs, reflecting a better antifungal activity. The behavior was more pronounced for FP-B which displayed the highest porating activity when tested on liposomes composed of mixtures of PC and SM in a 1 : 1 molar ratio.

FPs were hemolytic on HRBCs with an activity of the same order of magnitude as other peptins, like SP25A, SP22A [11,14] and Tol [20], as reported in Table 1. Interestingly, as already observed within some groups of LDPs [14], the effects increased with the length of the FPs' fatty acid moiety. Indeed FP-B, carrying a hydroxydecanoyl chain, was 3 times more active on HRBC than FP-A, with a hydroxyoctanoyl acid

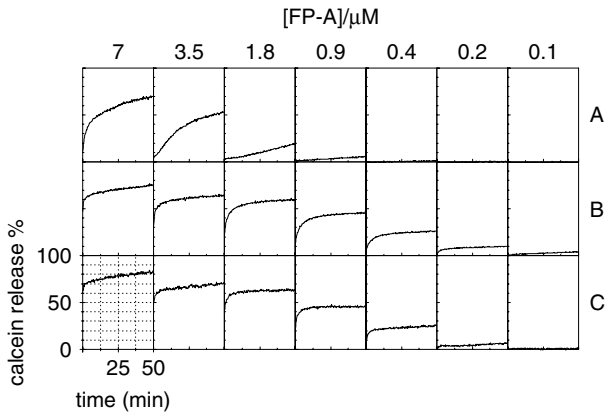

Figure 2 Calcein release kinetics of FP-A from LUVs composed of PC : Cho (50 : 50) (row A), PC : SM (50 : 50) (row B) and PC (row C). [Lipid] = 6–8 μM. [FP-A] = 7 μM in the first column, diluted by 2-fold steps along each row. Fluorescence intensities were monitored every 15 s with a microplate reader (λex = 485 nm and λem = 590 nm), for 50 min at room temperature. Scales are indicated on the bottom left panel.

DOI: 10.1002/psc

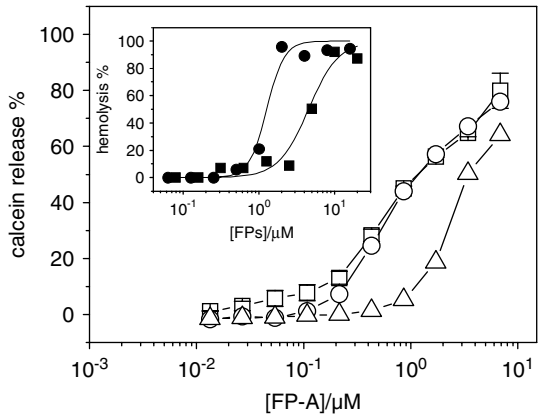

Figure 3 Percentage of membranolytic activity on LUVs and HRBCs as a function of FPs concentration. Main panel: Calcein release activity on LUVs of PC : Cho (50 : 50) (Δ), PC : SM (50 : 50) (□) and PC (○). Experimental conditions as in Figure 2. Inset: Hemolytic activity of both FP-A (■) and FP-B (●) on HRBCs. Cells/well = 2.4×10^6. Absorbance was measured at 650 nm, every 9 s with a microplate reader for 45 min at room temperature.

Table 1 Comparison of membrane damage activity due to FPs and other LDPs on LUVs of different lipid composition and on HRBCs

	Activity $1/C_{50}$ (μM^{-1})[a]					
	FP-A	FP-B	SP25A	SP22A	Tol	SRE
LUVs permeabilization[b]						
PC	0.8	0.5	0.4[c]	3.8[c]	2.8[d]	0.1[c]
PC : SM (50 : 50)	0.8	1.3	2.5[c]	4.2[c]	4.9[d]	1.1[c]
PC : Cho (50 : 50)	0.3	0.2	0.1[c]	0.5[c]	1.0[d]	20.0[c]
Hemolysis						
HRBCs	0.3	0.9	0.3[c]	0.1[c]	0.1[e]	1.6[c]

[a] C_{50} is defined as the peptide concentration causing 50% of activity, either calcein release from LUVs or hemolysis. Standard deviations for the reported $1/C_{50}$ values were less than 8–12%.
[b] Lipid mixtures are reported on a molar basis.
[c] Data from [14].
[d] Data from [15].
[e] Data from [20].

(Figure 3 inset and Table 1). This structural–functional correlation could explain also the highest activity found for FP-B with respect FP-A in physiological experiments [9]. On liposomes the difference in activity between the two FPs was less pronounced and was modulated by the lipid composition (Table 1).

Planar Lipid Membrane Experiments

The addition of FPs to the bathing solution at one side of a POPC membrane induced discrete increases of the ionic current through the bilayer, indicating the formation of ionic channels (Figure 4). FP-B was again more active than FP-A, since a lower concentration of FP-B (3–10 nM) was enough to elicit the same total current observed with 40 nM FP-A. The current steps induced by FP-B in 100 mM KCl showed an average conductance of 3.1 ± 0.4 pS and 9.1 ± 1.4 pS at −140 and +140 mV, respectively (Figure 4). These values were similar to those reported for cormycin from *P. corrugata* [21] but smaller than those of the other LDPs so far characterized, e.g. SP25A, SP22A, SRE, and ST, which are in the range of 20–40 pS [22–27].

As expected from the homology of their peptidic sequence, FP-B and FP-A formed channels with similar properties. Indeed, the single channel conductance at different voltages was the same for both FPs, into the experimental error (Figure 5). The resulting current voltage curve was nonlinear, with a pore conductance always larger at positive voltages than at the corresponding negative voltages (Figure 5). By extrapolation, the intercept passed through the origin as expected from the symmetry of the bathing solutions used. The nonlinearity of the single channel current/voltage curve is a common property of the LDPs ([22,23,26]) and is conceivable in the asymmetric distribution of the fixed charges along the pore lumen which influence the local ion concentration [13]. This nonlinearity remained throughout the duration of the

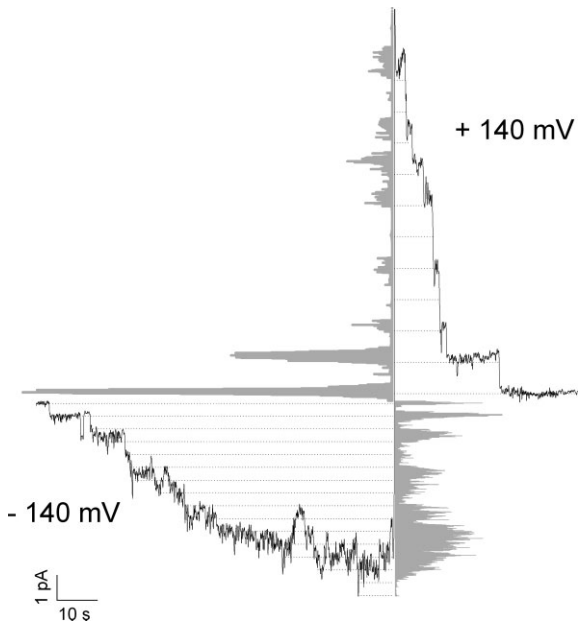

Figure 4 Single channel current fluctuations induced by 3 nM FP-B (added on the *cis*-side) under an applied voltage of ±140 mV, as indicated. The occupation histograms associated to the reported traces disclosed two conductance levels, i.e. 3.1 ± 0.4 pS and 9.1 ± 1.4 pS, at negative and positive potentials respectively. The electrolyte on both sides of a POPC bilayer was 100 mM KCl, 10 mM Mes, pH 6. Experiments were done at room temperature.

DOI: 10.1002/psc

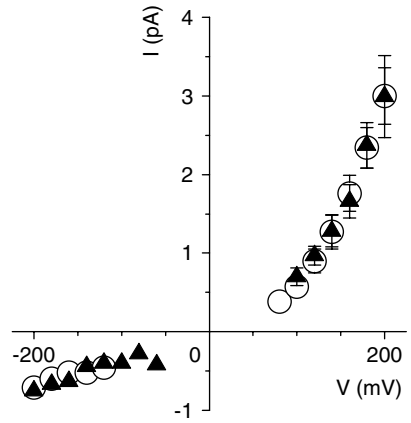

Figure 5 Voltage dependence of single channel ionic current through FP-A (○) or FP-B (▲) pore. Values are averages obtained from the records of single channel activity from experiments similar to that of Figure 4. The electrolyte on both sides of a POPC bilayer was 100 mM KCl, 10 mM Mes, pH 6. [FP-A] = 40 nM and [FP-B] = 3 –10 nM.

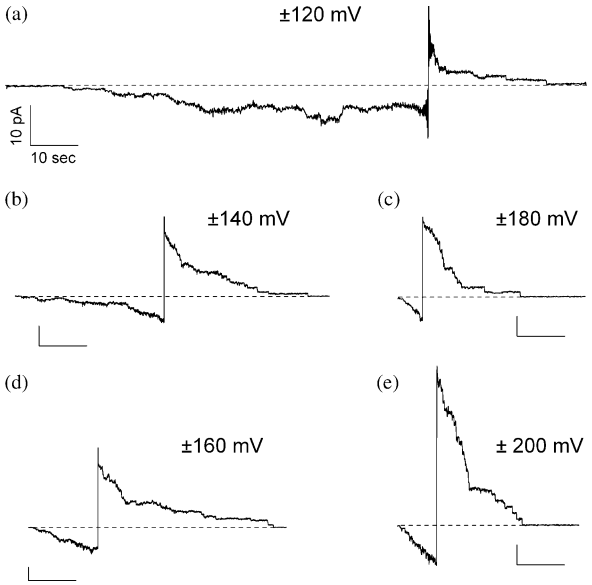

Figure 6 Records of transmembrane current of POPC bilayers containing FP-A (added on the *cis*-side) before and after the reversal of the applied electric field. (a) ±120 mV; (b) ±140 mV; (c) ±160 mV; (d) ±180 mV; (e) ±200 mV. Scales are reported in (a) and are the same for all panels. Other experimental conditions are as in Figure 5.

experiment (i.e. few hours) suggesting that FPs, which carry a net positive charge on the lactone ring (Figure 1), were inserted and oriented in the same direction in PLM and did not undergo any reorientation.

FPs' channels showed a voltage-dependent behavior: pore opening was stimulated by *cis*-negative voltage while a switch to the positive one resulted in an immediate channels closure (Figure 4). We assessed this behavior, i.e. the 'gating' of the pore [28] at different voltages, by performing field reversal experiments (Figure 6).

The transmembrane current of a POPC bilayer containing FPs (either FP-A or FP-B) was recorded before and after the reversal of the applied electric fields. For all the potentials tested (from ±120 to ±200 mV, at step of 20 mV), switching the potential from negative to positive voltages induced an increase in the absolute value of transmembrane current with a simultaneous decrease in the number of open channels. Similarly to other LDPs [22,26] high values of applied potentials were necessary for channel openings, possibly depending on the lipid composition used [29]. As shown in Figure 6, the rate of increase (or decrease) in the total current grew with the absolute value of the applied potential. This voltage dependence of FPs' channel openings was very similar to that already described for SP25A, SP22A and tolaasin among peptins [22,23,30,31], and for SRE and ST in the group of nonapeptides [26,27]. This behavior could be interpreted with the same two-state model proposed for SP25A [22]: the transition between the open and the closed state is due to a major conformational change that involves the LDP inserted in the membrane and is induced by the movement of the charged cyclic peptide moiety by switching electric field. According to that model, application of a negative voltage might favor the opening of the pore by attracting the positive charges out of the membrane and inducing an elongation of the acylated hydrophobic peptide chain to span completely the hydrophobic core of the membrane [22].

Similarly to the behavior of SP25A [22], SP22A [23], SRE, [25] and ST [27], additional voltage-dependent fluctuations of smaller size were also observed in the FPs' single channel traces. These fluctuations were more pronounced at negative potentials, and disappeared at positive applied voltages much faster than the main pores. As in the case of SP25A [22], the number of small pores opened increased gradually with the number of large pores during the initial incorporation (Figure 4).

To complete the characterization of FPs' channels we determined their cation–anion selectivity by measuring the reversal potential (V_{rev}). A 10-fold transmembrane concentration gradient of KCl (0.1 M KCl at *cis*-side and 1 M KCl at *trans* side) was formed across the bilayer in the presence of FP-A, and the measured potential necessary to zero the current (V_{rev}) corresponded to +13.5 mV for both FPs. Surprisingly, this value indicates weak cation selectivity, with a permeability ratio of cations over anions (P^+/P^-) of 2.1.

Such selectivity could not be interpreted in terms of any simplicistic electrostatic attraction models, in fact FPs have a net double positive charge, provided by the two Dab residues located at the cyclic peptide moiety, which should attract anions and therefore display an anionic selectivity. This was indeed the case for other related LDPs so far analyzed, like SRE [23–26,32] and

DOI: 10.1002/psc

SP25A [22]. Nevertheless, cationic selectivity seems to be a common characteristic of positively charged channel forming peptides, like mastoparan and mast cell degranulation peptide [33,34], the antimicrobial cathelicidin tritrpticin [35], gaegurin from frog skin [36], synthetic basic α-helical peptides [37], a segment of the sodium channel polypeptide [38] (see also the excellent review of Sansom [33], and that more recent of Kourie [39]).

Interestingly, also Tol which is positively charged, shows cation selectivity [30]. It shares with FPs a contraction of the lactone ring to five residues; this difference in charge density with respect to the other LDPs (whose number of residues involved is nine for nonapeptides or eight for the other peptins) could lead to a different concentration of counter ions which reflects a modified involvement of the cyclic peptide moiety in the channel structure with consequences on selectivity and on conductivity (indeed FPs had a conductance at least 3-fold smaller than SP25A).

CD and NMR spectroscopy revealed that FPs are completely unstructured in aqueous solution with a large molecular flexibility, while in a membrane mimetic solution the peptidic region appears to adopt a helical structure [40]. These results are in line with those reported for Tol where a prevalence of helical structure was indeed observed in lipid membrane [15]. According to the main model proposed for the mechanism of action of several α-helical peptides, known as the Shai-Matsuzaki-Huang model [41], lipid molecules could participate in the formation of the lesion and cooperate with the peptide to the polar surface of the pore. In this way, the selectivity of the resulting lipidic and peptidic pore could be modulated by the presence of phospholipid heads as constituent of the channel lumen. This type of pore (known as toroidal pore) has been recently proposed for other LDPs like SRE [32] and SP22A [42] and could contribute to a better explanation of some differences in electrical behavior.

CONCLUSIONS

Similarly to other LDPs so far characterized, FPs showed a lytic activity on both synthetic and biological membranes. By using the PLM technique, we were able to demonstrate that FP-A and FP-B formed ion channels with similar properties on membranes composed of POPC. We presented here for the first time, a preliminary characterization of these channels in terms of conductance, voltage-dependency, and selectivity.

Acknowledgements

We thank prof. A. Ballio for providing the culture filtrates of *P. fuscovaginae*. This work was financially supported by Provincia Autonoma di Trento (PAT, project SyrTox) and by Fondazione Cassa di Risparmio di Trento e Rovereto.

REFERENCES

1. Ballio A, Bossa F, Camoni L, Di Giorgio D, Flamand MC, Marcite H, Nitti G, Pucci P, Scaloni A. Structure of fuscopeptins, phytotoxic metabolites from *Pseudomonas fuscovaginae*. *FEBS Lett.* 1996; **381**: 213–216.
2. Ballio A, Barra D, Bossa F, Collina A, Grgurina I, Marino G, Moneti G, Paci M, Pucci P, Segre A, Simmaco M. Syringopeptins, new phytotoxic lipodepsipeptides of *Pseudomonas syringae* pv. *syringae*. *FEBS Lett.* 1991; **291**: 109–112.
3. Grgurina I. Toxicity of syringomycins and its pathological significance. In *Advances in Microbial Toxin Research and its Biotechnological Exploitation*, Upadhyay RK (ed.). Kluwer Academic: New York, 2002; 105–140.
4. Nutkins JC, Mortishire-Smith RJ, Packman LC, Brodey CL, Rainey PB, Johnstone K, Williams DH. Structure determination of tolaasin, an extracellular lipodepsipeptide produced by the mushroom pathogen *Pseudomonas tolaasii* Paine. *J. Am. Chem. Soc.* 1991; **113**: 2621–2627.
5. Bassarello C, Lazzaroni S, Bifulco G, Lo Cantore P, Iacobellis NS, Riccio R, Gomez-Paloma L, Evidente A. Tolaasins A-E, five new lipodepsipeptides produced by *Pseudomonas tolaasii*. *J. Nat. Prod.* 2004; **67**: 811–816.
6. Emanuele MC, Scaloni A, Lavermicocca P, Jacobellis NS, Camoni L, Di Giorgio D, Pucci P, Paci M, Segre A, Ballio A. Corpeptins, new bioactive lipodepsipeptides from cultures of *Pseudomonas corrugata*. *FEBS Lett.* 1998; **433**: 317–320.
7. Segre A, Bachmann RC, Ballio A, Bossa F, Grgurina I, Iacobellis NS, Marino G, Pucci P, Simmaco M, Takemoto JY. The structure of syringomycins A1, E and G. *FEBS Lett.* 1989; **255**: 27–31.
8. Fukuchi N, Isogai A, Nakayama J, Takayama S, Yamashita S. Isolation and structural elucidation of syringostatins, phytotoxins produced by *Pseudomonas syringae* pv. *syringae* lilac isolate. *J. Chem. Soc., Perkin Trans.* 1992; **1**: 875–880.
9. Batoko H, d'Exaerde AD, Kinet JM, Bouharmont J, Gage RA, Maraite H, Boutry M. Modulation of plant plasma membrane H^+-ATPase by phytotoxic lipodepsipeptides produced by the plant pathogen *Pseudomonas fuscovaginae*. *Biochim. Biophys. Acta-Biomembr.* 1998; **1372**: 216–226.
10. Flamand MC, Pelsser S, Ewbank E, Maraite H. Production of syringotoxin and other bioactive peptides by *Pseudomonas fuscovaginae*. *Physiol. Mol. Plant Pathol.* 1996; **48**: 217–231.
11. Dalla Serra M, Fagiuoli G, Nordera P, Bernhart I, Della Volpe C, Di Giorgio D, Ballio A, Menestrina G. The interaction of lipodepsipeptide toxins from *Pseudomonas syringae* pv. *syringae* with biological and model membranes: a comparison of syringotoxin, syringomycin and syringopeptins. *Mol. Plant-Microbe Interact.* 1999; **12**: 391–400.
12. Alvarez C, Dalla Serra M, Potrich C, Bernhart I, Tejuca M, Martinez D, Pazos IF, Lanio ME, Menestrina G. Effects of lipid composition on membrane permeabilization by Sticholysin I and II, two cytolysins of the sea anemone *Stichodactyla helianthus*. *Biophys. J.* 2001; **80**: 2761–2774.
13. Dalla Serra M, Menestrina G. Characterisation of molecular properties of pore-forming toxins with planar lipid bilayers. In *Bacterial Toxins, Methods and Protocols*, Holst O (ed.). Humana Press: Totowa, NJ, 2000; 171–188.
14. Menestrina G, Coraiola M, Fogliano V, Fiore A, Grgurina I, Carpaneto A, Gambale F, Dalla Serra M. Antimicrobial lipodepsipeptides from *Pseudomonas* Spp: a comparison of their activity on model membranes. In *Pseudomonas Syringae and Related Pathogens. Biology and Genetic*, Iacobellis SN (ed.). Kluwer Academic Publishers: Dordrecht, NL, 2003; 185–198.
15. Coraiola M, Lo Cantore P, Lazzaroni S, Evidente A, Iacobellis NS, Dalla Serra M. Tolaasin I and WLIP, lipodepsipeptides from *Pseudomonas tolaasii* and *P. "reactans"*, permeabilize model membranes. *Biochim. Biophys. Acta-Biomembr.* 2006; **1758**: 1713–1722.

16. Bender CL, Alarcon Chaidez F, Gross DC. *Pseudomonas syringae* phytotoxins: Mode of action, regulation, and biosynthesis by peptide and polyketide synthetases. *Microbiol. Mol. Biol. Rev.* 1999; **63**: 266–292.
17. Julmanop C, Takano Y, Takemoto JY, Miyakawa T. Protection by sterols against the cytotoxicity of syringomicin in the yeast *Saccharomyces cerevisiae*. *J. Gen. Microbiol.* 1993; **139**: 2323–2327.
18. Taguchi N, Takano Y, Julmanop C, Wang Y, Stock S, Takemoto JY, Miyakawa T. Identification and analysis of the *Saccharomyces cerevisiae* SYR1 gene reveals that ergosterol is involved in action of syringomycin. *Microbiology* 1994; **140**: 353–359.
19. Feigin AM, Schagina LV, Takemoto JY, Teeter JH, Brand JG. The effect of sterols on the sensitivity of membranes to the channel-forming antifungal antibiotic, syringomycin E. *Biochim. Biophys. Acta-Biomembr.* 1997; **1324**: 102–110.
20. Lo Cantore P, Lazzaroni S, Coraiola M, Dalla Serra M, Cafarchia C, Evidente A, Iacobellis NS. Biological Characterisation of WLIP produced by *Pseudomonas reactans* strain NCPPB1311. *Mol. Plant-Microbe Interact.* 2006; **19**: 1113–1120.
21. Scaloni A, Dalla Serra M, Amodeo P, Mannina L, Vitale RM, Segre AL, Cruciani O, Lodovichetti F, Greco ML, Fiore A, Gallo M, D'Ambrosio C, Coraiola M, Menestrina G, Graniti A, Fogliano V. Structure, conformation and biological activity of a novel lipodepsipeptide from *Pseudomonas corrugata*: Cormycin A. *Biochem. J.* 2004; **384**: 25–36.
22. Dalla Serra M, Nordera P, Bernhart I, Di Giorgio D, Ballio A, Menestrina G. Conductive properties and gating of channels formed by syringopeptin 25-A, a bioactive lipodepsipeptide from *Pseudomonas syringae* pv. *syringae*, in planar lipid membranes. *Mol. Plant-Microbe Interact.* 1999; **12**: 401–409.
23. Agner G, Kaulin YA, Gurnev PA, Szabo Z, Schagina LV, Takemoto JY, Blasko K. Membrane-permeabilizing activities of cyclic lipodepsipeptides, syringopeptin 22A and syringomycin E from *Pseudomonas syringae* pv. *syringae* in human red blood cells and in bilayer lipid membranes. *Bioelectrochemistry* 2000; **52**: 161–167.
24. Schagina LV, Kaulin YA, Feigin AM, Takemoto JY, Brand JG, Malev VV. Properties of ion channels formed by the antibiotic syringomycin E in lipid bilayers: dependence on the electrolyte concentration in the bathing solution. *Biol. Membrany* 1998; **15**: 433–446.
25. Kaulin YA, Schagina LV, Bezrukov SM, Malev VV, Feigin AM, Takemoto JY, Teeter JH, Brand JG. Cluster organization of ion channels formed by the antibiotic syringomycin E in bilayer lipid membranes. *Biophys. J.* 1998; **74**: 2918–2925.
26. Feigin AM, Takemoto JY, Wangspa R, Teeter JH, Brand JG. Properties of voltage-gated ion channels formed by syringomycin E in planar lipid bilayers. *J. Membr. Biol.* 1996; **149**: 41–47.
27. Szabo Z, Grof P, Schagina LV, Gurnev PA, Takemoto JY, Matyus E, Blasko K. Syringotoxin pore formation and inactivation in human red blood cell and model bilayer lipid membranes. *Biochim. Biophys. Acta-Biomembr.* 2002; **1567**: 143–149.
28. Hille B. *Ionic Channels of Excitable Membranes*. Sinauer Associates Publishers: Sunderland, MA, 1992.
29. Carpaneto A, Dalla Serra M, Menestrina G, Fogliano V, Gambale F. The phytotoxic lipodepsipeptide syringopeptin 25A from *Pseudomonas syringae* pv *syringae* forms ion channels in sugar beet vacuoles. *J. Membr. Biol.* 2002; **188**: 237–248.
30. Brodey CL, Rainey PB, Tester M, Johnstone K. Bacterial blotch disease of the cultivated mushroom is caused by an ion channel forming lipodepsipeptide toxin. *Mol. Plant-Microbe Interact.* 1991; **4**: 407–411.
31. Cho KH, Kim YK. Two types of ion channel formation of tolaasin, a *Pseudomonas* peptide toxin. *FEMS Microbiol. Lett.* 2003; **221**: 221–226.
32. Malev VV, Schagina LV, Gurnev PA, Takemoto JY, Nestorovich EM, Bezrukov SM. Syringomycin E channel: a lipidic pore stabilized by lipopeptide? *Biophys. J.* 2002; **82**: 1985–1994.
33. Sansom MSP. The biophysics of peptide models of ion channels. *Prog. Biophys. Mol. Biol.* 1991; **55**: 139–235.
34. Ide T, Taguchi T, Morita T, Sato M, Ikenaka K, Aimoto S, Kondo T, Hojo H, Kasai M, Mikoshiba K. Mast cell degranulating peptide forms voltage gated and cation-selective channels in lipid bilayers. *Biochem. Biophys. Res. Commun.* 1989; **163**: 155–160.
35. Salay LC, Procopio J, Oliveira E, Nakaie CR, Schreier S. Ion channel-like activity of the antimicrobial peptide tritrpticin in planar lipid bilayers. *FEBS Lett.* 2004; **565**: 171–175.
36. Kim HJ, Han SK, Park JB, Baek HJ, Lee BJ, Ryu PD. Gaegurin 4, a peptide antibiotic of frog skin, forms voltage-dependent channels in planar lipid bilayers. *J. Pept. Res.* 1999; **53**: 1–7.
37. Anzai K, Hamasuna M, Kadono H, Lee S, Aoyagi H, Kirino Y. Formation of ion channels in planar lipid bilayer membranes by synthetic basic peptides. *Biochim. Biophys. Acta-Biomembr.* 1991; **1064**: 256–266.
38. Tosteson MT, Auld DS, Tosteson DC. Voltage-gated channels formed in lipid bilayers by a positively charged segment of the Na-channel polypeptide. *Proc. Natl. Acad. Sci. U.S.A.* 1989; **86**: 707–710.
39. Kourie JI, Shorthouse AA. Properties of cytotoxic peptide-formed ion channels. *Am. J. Physiol. Cell Physiol.* 2000; **278**: C1063–C1087.
40. Baré S, Coiro VM, Scaloni A, DiNola A, Paci M, Segre AL, Ballio A. Conformations in solution of the fuscopeptins – phytotoxic metabolites of *Pseudomonas fuscovaginae*. *Eur. J. Biochem.* 1999; **266**: 484–492.
41. Zasloff M. Antimicrobial peptides of multicellular organisms. *Nature* 2002; **415**: 389–395.
42. Szabo Z, Budai M, Blasko K, Grof P. Molecular dynamics of the cyclic lipodepsipeptides' action on model membranes: effects of syringopeptin 22A, syringomycin E, and syringotoxin studied by EPR technique. *Biochim. Biophys. Acta-Biomembr.* 2004; **1660**: 118–130.

DOI: 10.1002/psc